

R. I. Didus, D. V. Myroniuk, L. A. Myroniuk, A. I. Ievtushenko

Features of technological synthesis and properties of ZnO-Cd based materials for photocatalytic applications. Review

*I.M. Frantsevich Institute for Problems of Materials Science, National Academy of Sciences of Ukraine,
3 Krzhyzhanovsky Str., 03142, Kyiv, Ukraine, romanik619@gmail.com*

Abstract: In this review, the current state of ZnO-Cd based materials for photocatalytic applications is summarized. Relevant technological synthesis methods such as pulsed laser deposition, magnetron sputtering, electrodeposition, sol-gel, metalorganic chemical vapor deposition, evaporating, spray pyrolysis, reflux are considered, and recent developments in effective and reproducible synthesis technology of nano- and microstructured zinc oxide, doped with cadmium and solid solutions of $Zn_{1-x}Cd_xO$ for photodecomposition of organic pollutant molecules are discussed. The synthesis technology and level of Cd doping has a significant effect on the structure and morphology of zinc oxide and, as a result, on the optical and photocatalytic properties. The figures of merit, the theoretical limitations and rational control of the concentration of the cadmium alloying impurity is necessary to create a material with balanced optical properties and photocatalytic activity. Lastly, the importance of doping ZnO by isovalent Cd impurity significantly improves its photocatalytic properties due to a narrowing of the band gap, a decrease in the rate of recombination of electron-hole pairs, which increases the efficiency of spatial charge separation, the formation of active oxide radicals and an increase in the specific surface area. Thus, ZnO-Cd based materials are the most promising photocatalytic materials for organic pollutants.

Keywords: zinc oxide; cadmium doping; morphology; nanostructures; optical properties; photocatalysis.

Received 26 December 2023; Accepted 23 March 2023.

Introduction

Toxic organic air and water pollutants pose a significant danger to both human health and the eco-fauna as a whole. In this regard, the development of the latest environmental technologies for quick and safe deactivation of organic pollutants is a particularly relevant scientific task. Currently, the main efforts of the world scientific community are focused on the development of photocatalysis technology as a highly productive process of decomposition of organic compounds under the influence of light. Therefore, the realization of a reliable and reproducible synthesis of materials with high photocatalytic properties becomes important.

Due to its unique physico-chemical properties, biocompatibility and availability of synthesis methods, wide bandgap (~ 3.3 eV) zinc oxide is one of the most promising photocatalytic materials of the future [1]. Due to its multifunctional properties, ZnO is promising for use

in solar cells, medical equipment, automotive industry, semiconductor industry, optoelectronics, biomaterials and for photocatalytic applications [2,3,4,5,6]. From an industrial point of view, ZnO is considered a very important material due to a number of advantages, such as low production cost, efficiency and non-toxic catalyst and environmental safety [7]. ZnO has high radiation resistance, good thermal properties, structural stability, biological compatibility, and effective optical absorption in the UV range [8]. It can be doped with impurity elements to obtain films with high conductivity and optical transparency [9,10]. However, the main disadvantage of zinc oxide is that this semiconductor material is able to effectively absorb light exclusively in the ultraviolet region of the optical spectrum, which significantly limits its use for photocatalysis.

Over the past 20 years, researchers have studied the alloying effect of Cd, Cu, Mg, Mn, Ni in zinc oxide on its optical properties. Among the above-mentioned alloying

elements, especially Cd provides the smallest bandgap value in the material, so it has many applications in industry and the environment protection. Bandgap tuning is desirable for wavelength stability and achieving a bandgap that matches the visible spectrum. Mosquera et al. [11] found that the band gap decreased from 3.21 eV to 3.11 eV as the evidence of influence Cd on the sample increased. With the correct Zn/Cd ratio, the band gap can be reduced to 2.92 eV [12,13,14].

I. Technological methods of synthesis of ZnO-Cd thin films (nanomaterials)

To date, several research articles have been published on the synthesis of the ZnO-Cd system using a variety of deposition methods, such as pulsed laser deposition (PLD) [5,15,16,17,18,19], electrodeposition [20,21,22], hydrothermal synthesis [21,20], sol-gel process [11,12,22,20,21,22,23,24], direct current [13,14,25] and radiofrequency magnetron deposition [27,28], spray pyrolysis (SP) [3,22,26,27,28,29], thermal co-evaporation [22, 36], molecular beam epitaxy (MBE) [2,5,36], remote

plasma-enhanced metalorganic chemical vapor deposition (RPE-MOCVD) [5,37,38], ion layering (SILAR) [34,39], spin-coating [4,40] and even reflux method [42] (Fig. 1, 2).

The article [22] describes the production of ZnO-Cd films by the SP method. This method is based on the preparation of homogeneous precursor solutions from salts, thin films of which are deposited on preheated substrates (Fig. 3). During the processes of deposition of thin oxide film, both chemical and thermal reactions occur. Using SP, relatively uniform films are grown with very high growth rates of the order of several hundreds of nanometers per minute. Therefore, it is an attractive and widely used method in industry for covering large areas.

Among the listed methods, sol-gel is a simple and suitable for large-area deposition method, which is usefulness for almost any transparent conductive films. The spin-coating technique is simple, as it does not require a vacuum or high temperature to deposit the films. The technology of films deposition by this method is shown in Fig. 4.

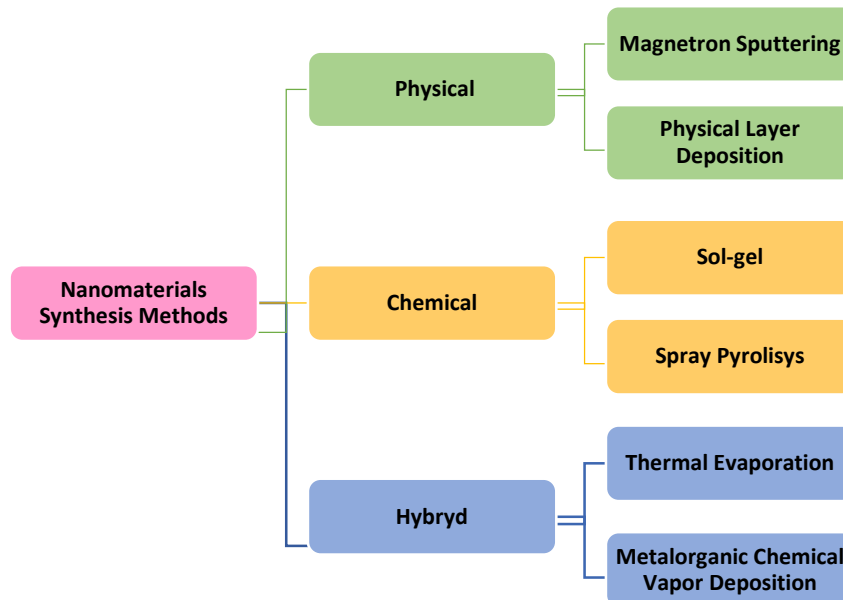


Fig. 1. General scheme of nanomaterial synthesis methods [43].

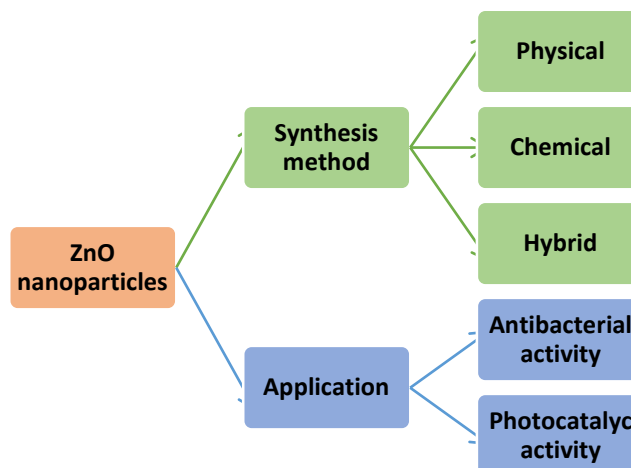


Fig.2. Synthesis methods of zinc NPs and their potential use [43].

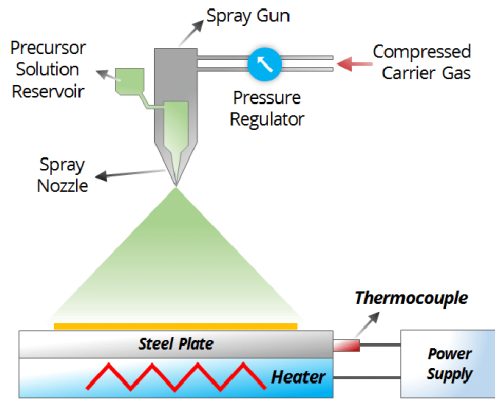


Fig. 3 Scheme of the installation for obtaining thin films by the spray pyrolysis method [22].

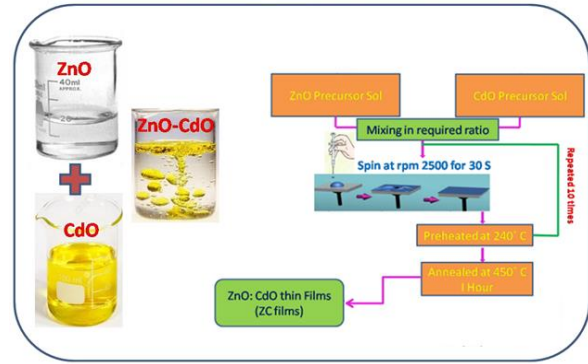


Fig. 4. Block diagram of deposition of ZnO:CdO sol-gel thin films by the spin-coating method [27].

II. Physical properties of thin films of the ZnO-Cd system

2.1. Microstructure and chemical composition of ZnO-Cd thin films.

The article [43] proposes growing nanostructures (NS) by the evaporation method on anodic aluminum oxide (AOA) substrates with gold (Au) particles deposited on it. SEM images of the obtained NS are shown at Fig. 5.

It was established that temperature is a key factor in the morphology of catalytically grown ZnO NS. At the higher temperature (700 °C), only ZnO nanowires were formed. At the lower temperature (680 °C) nanobelts appeared. ZnO nanocombs were formed when the temperature was 660 °C.

Undoped and doped ZnO samples (Fig. 6) with different doping concentrations (1–5% by weight of Cd) are labeled CZO-0, CZO-1, CZO-2, CZO-3, CZO-4, and CZO-5, respectively. Sample CZO-0 deposited at 450 °C

on a glass substrate (Fig. 6, a), consists of various tiny spherical grains. A similar morphology is observed for sample CZO-1. For the CZO-2 sample, the morphology of which is shown in Fig. 6, c, the grain density is higher, and the grain size is 50 nm. Surface morphology changes with 3 % Cd doping (Fig. 6, d). Agglomeration of grains is observed on the surface of CZO-3 films. With a higher cadmium doping of CZO-4 and CZO-5 samples, a smooth surface covered with many spherical grains of 80-100 nm in size was observed. Among all the samples, the CZO-2 film shows a well-distributed granular morphology [40].

SEM images presented in the article [39] for undoped and Cd-doped ZnO films are shown in Fig. 7. It can be seen from this figure that the surface of the zinc oxide film is rough and consists of large and faceted grains (Fig. 7, a), and the thin ZnO-Cd film consists of almost hexagonal crystallites, mainly oriented perpendicular to the surface of the substrate, that is, along the *c* axis (Fig. 7, b). This change in the shape of the grains is probably related to the inclusion of cadmium, which disrupts the arrangement of atoms.

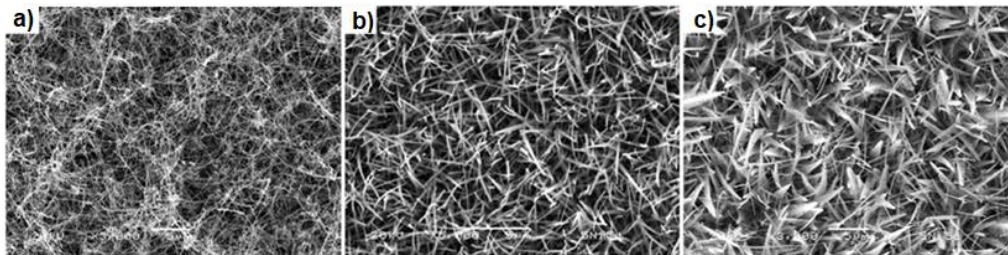


Fig. 5. SEM images of ZnO NS grown on substrates filled with Au particles at: a – 700 °C; b – 680 °C; c - 660 °C [44].

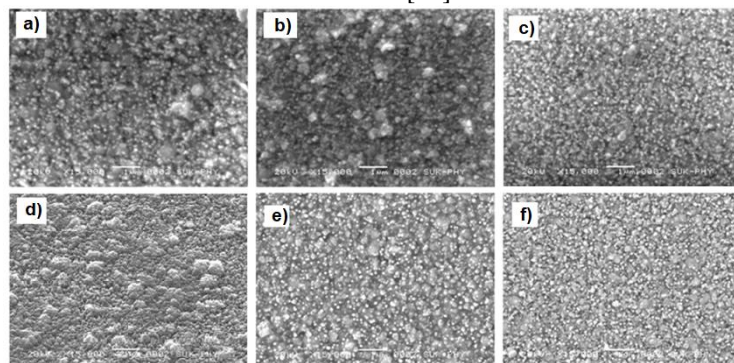


Fig. 6. SEM images of Cd-ZnO thin films deposited by pyrolysis sputtering with different concentrations of Cd doping: a – CZO-0; b – CZO-1; c – CZO-2; d – CZO-3; e – CZO-4; f – CZO-5 [40].

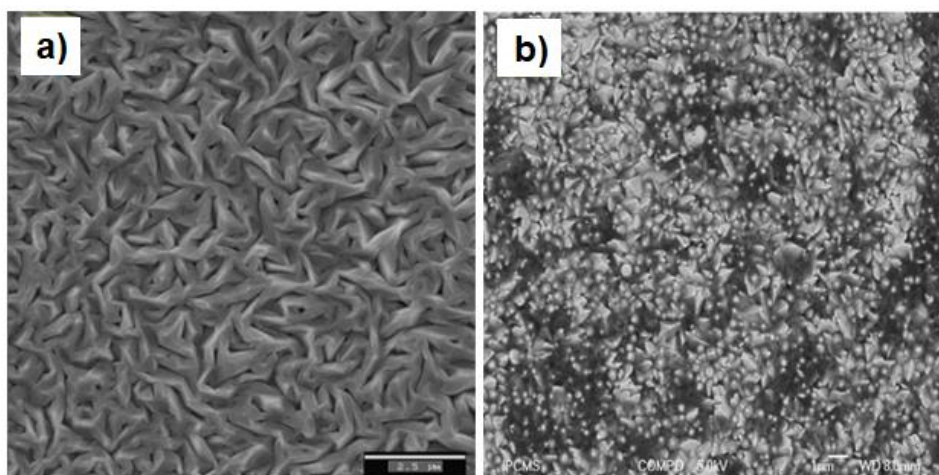


Fig. 7. SEM images of thin films: a – ZnO; b – ZnO-Cd [39].

The authors [42] synthesized ZnO and ZnO-Cd nanoparticles by the reflux method. ZnO nanoparticles were obtained, as well as nanoparticles with 5 % and 10 % by weight fraction of cadmium doping.

In Fig. 8 shows X-ray patterns of synthesized undoped ZnO and doped ZnO with different Cd content. All the obtained peaks are in good agreement with the hexagonal crystal structure of ZnO. No other impurity peak was observed in the X-ray pattern, indicating ZnO nanocrystals that have a pure hexagonal crystal structure. No impurity peaks were observed. The observed ZnO diffraction reflections appear at 31.71 °, 34.41 °, 36.24 °, 47.52 °, 56.6 °, 62.8 °, 66.3 °, 67.9 °, 69.1 °, 72.4 ° and 76.9 ° and correspond to the orthogonal planes (100), (002), (101), (110), (103), (200), (112), (201), (004) and (202), respectively.

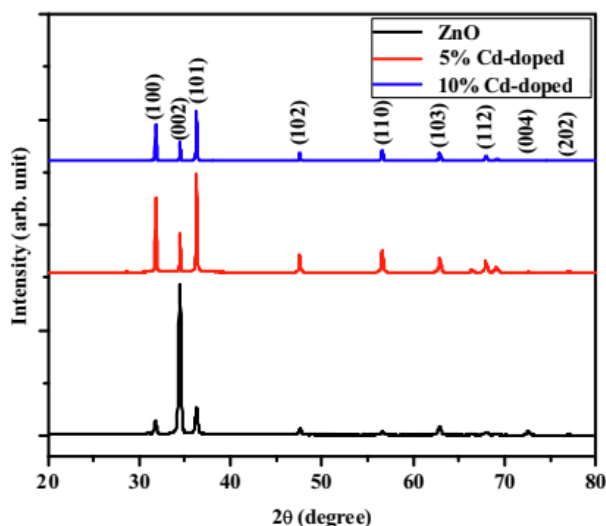


Fig. 8. Combined X-ray patterns of synthesized thin films [42].

An increase in the Cd content causes decreasing in the intensity of all diffraction peaks. This decrease is explained by the effect of defects created by cadmium ions included in the structure of the ZnO lattice. Compared to the pure ZnO film, the intensity of the (002) peak decreases for Cd-doped ZnO films, which is confirmed by the X-ray patterns in Figure 8. It is worth noting that the

relative intensity of the (101) peak increases for Cd-doped ZnO films. Thus, doping with cadmium leads to the loss of the predominant orientation along the *c* axis. These observations, combined with a decrease in the relative intensity of the (002) peak, confirm that the inclusion of Cd increases the degree of polycrystallinity of the films. Therefore, the synthesized nanocrystals retain a stable hexagonal ZnO phase.

The grain size of the samples was calculated using Scherrer's formula. The obtained crystallite sizes of the (002) plane of pure ZnO, ZnO doped with 5 % Cd, and the ZnO sample doped with 10 % Cd are 32.19, 48.23, and 57.94 nm, respectively. It is shown that doping with cadmium leads to an increase in the size of crystallites.

To investigate the overall morphology, the as-grown undoped and cadmium-doped ZnO nanoparticles were examined by SEM, and the results are shown in Fig. 9.

In Fig. 9, a, shown that undoped ZnO is synthesized in nanocrystalline structures of high density. The SEM image shows a polycrystalline morphology of nanocrystalline size with interconnected grains present on undoped ZnO nanoparticles. In Fig. 9, b shows highly agglomerated particles with a size of 400–500 nm for ZnO samples doped with 5 % Cd. It should be noted that the samples look like particles oriented in different directions. In Fig. 9, c shows highly agglomerated quasi-spherical particles with a size of 600–700 nm for a ZnO sample doped with 10 % Cd. Some of them connected together to form secondary particles derived from tiny particles with a high surface tendency to cluster. It is obvious that the crystallite size gradually increases with increasing Cd doping. The full array of one crystal structure is in the range of 2 μm [42].

Quite the opposite result, in contrast to those shown in Fig. 8 [42] demonstrated the samples synthesized in [35] by the SP method. The samples in this paper demonstrated an increase in the intensity of the (002) peak when doped with cadmium (Fig. 10). This behavior indicates a decrease in the level of crystallinity of the structure.

In Fig. 11 shows that the positions of the diffraction peaks systematically shift towards smaller angles with increasing cadmium concentration. This testifies to the successful replacement of Zn²⁺ by Cd²⁺ ions.

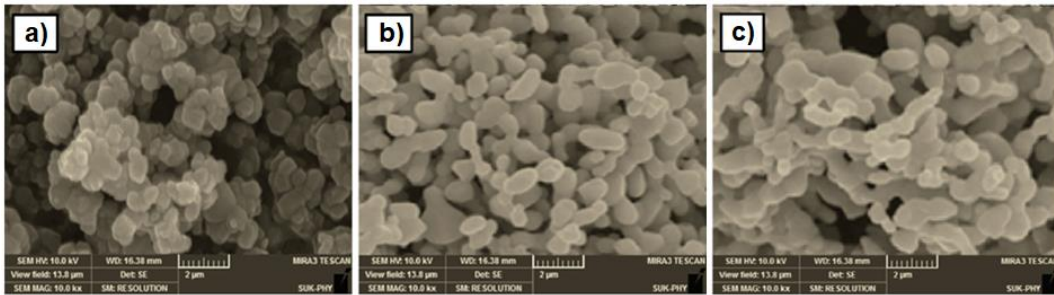


Fig.9. SEM photograph of nanoparticles synthesized by the method dephlegmation: a – undoped ZnO; b – ZnO doped with 5 % Cd; c – ZnO doped with 10 % Cd [42].

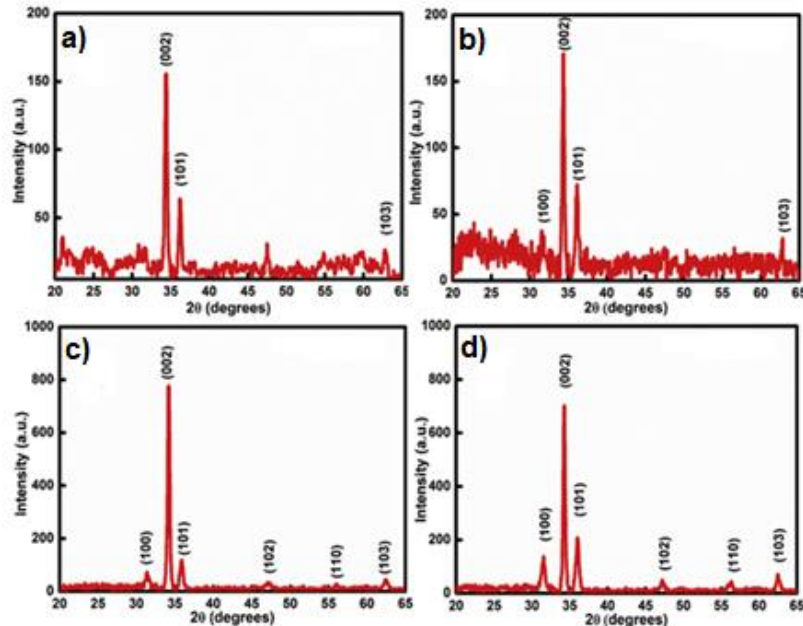


Fig. 10. X-ray diffraction of $Zn_{1-x}Cd_xO$ thin films with different atomic fractions of doping: a – 0%; b – 5%; c - 10 %; d – 20 % [35].

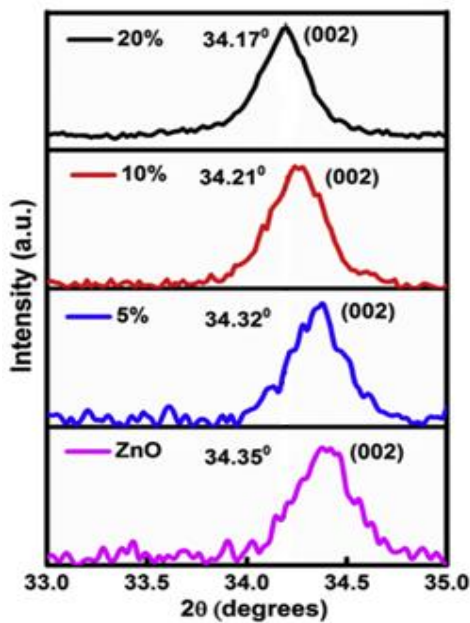


Fig. 11. Shift of the (002) peak position of $Zn_{1-x}Cd_xO$ when the level of cadmium doping changes [35].

The resulting structure was studied by SEM. The low-magnification image shows the uniformity of the formation of the microstructure without any holes or

cracks. At higher magnification, it can be observed that the film consists of densely packed and randomly arranged lamellar structures. When adding 5 molar Cd %, the surface is modified with grains of arbitrary shape, as shown in Fig. 12, b. Increasing the cadmium concentration to 10 and 20 molar % results in a thin films with a grainy morphology. This granularity in structures can be observed in Fig. 12, c,d . These results show that the concentration of cadmium changes the surface morphology of the films. The resulting structures are of great importance due to their high specific surface area and adsorption capacity. In general, SEM image in Fig. 12 can be called similar to the results shown in Fig. 7 [39].

2.2. Optical properties

Optical transmission spectra of Cd-doped ZnO thin films synthesized by the sol-gel method is considered in the article [28]. In Fig. 13 shows the transmission spectra of samples with different molar Cd %, as well as PL spectra.

The films are 198, 205, 180, and 140 nm thick with a cadmium weight fraction of 0 %, 0.45 %, 0.51 %, and 0.56 %, respectively. All films demonstrate transparency of 80-90 % in the visible and infrared regions of the spectrum. High transparency is associated with good structural homogeneity, crystallinity and thickness.

It was found that the transparency decreases if the

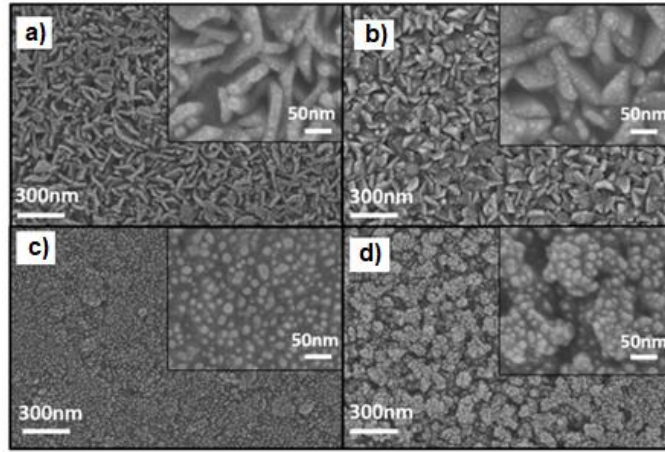


Fig. 12. SEM image of $Zn_{1-x}Cd_xO$ with different atomic fraction of doping: a) – 0 %; b) – 5 %; c) – 10 %; d) – 20 % [35].

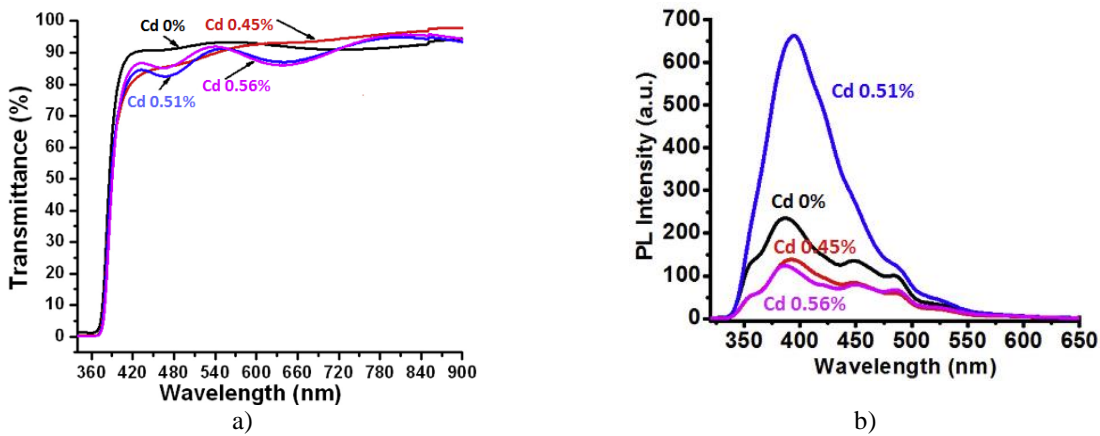


Fig. 13. Spectra of ZnO thin films with different levels of Cd doping: a) – optical transmission spectra; b) - PL spectra [28].

annealing temperature is more than 450 °C. On the optical transmission spectra at cadmium concentrations of 0.51 % and 0.56 % in Fig. 13, a, an interference pattern is observed, which is characteristic of thin films [16]. Also at 370 nm, a sharp absorption edge is observed, which shifts towards a higher wavelength with doping increasing. This red shift of the absorption edge indicates a decrease in the optical bandwidth of ZnO thin films [28].

PL excitation spectra were recorded for emission at 385 nm, equivalent to the optical transmission band of 3.22 eV of the ZnO film in this study. The corresponding photoluminescence spectra are shown in Fig. 13, b.

A similar PL spectrum is observed when studying the sample that was synthesized in [17] by the method of pulsed laser deposition on a quartz substrate.

Experimental PL spectra of $Zn_{1-x}Cd_xO$ with different concentrations of Cd are shown in Fig. 14. At Cd $x = 0.074$ and less, the near band edge (NBE) emission peak shows a red shift from 381 nm to 426 nm or from 3.252 eV to 2.908 eV. When the Cd concentration is further increased to 0.151, a very broad emission band extending from 400 nm to 530 nm in visible range of the PL spectra.

PL spectra of undoped and Cd-doped ZnO nanostructures synthesized by the evaporation method were measured and shown in Fig. 15 [44]. The curve in Fig. 15, a with the center of the emission band at 494 nm

and the curve in Fig. 15, b with the center at 505 nm refer to undoped ZnO samples and ZnO-Cd in accordance.

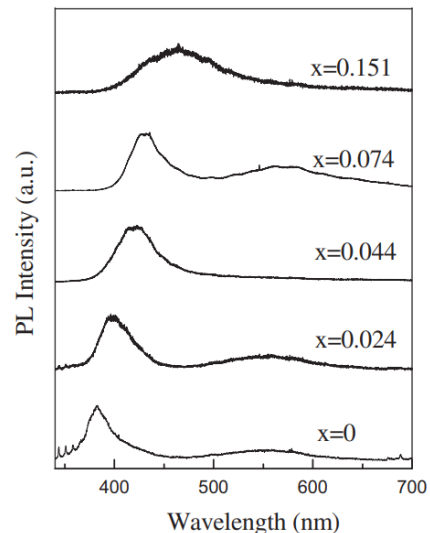


Fig. 14. PL spectra of $Zn_{1-x}Cd_xO$ films with different concentrations of Cd [17].

The green emission band around 500 nm arises as a result of the recombination of holes with electrons occupying a singly ionized oxygen vacancy. According to the PL emission band on the ZnO curve, the emission band

of ZnO nanostructures doped with cadmium has a red shift. In opposite to [17] at [28], no emission in the 375 nm region was detected, which could be a consequence of the high density of oxygen vacancies.

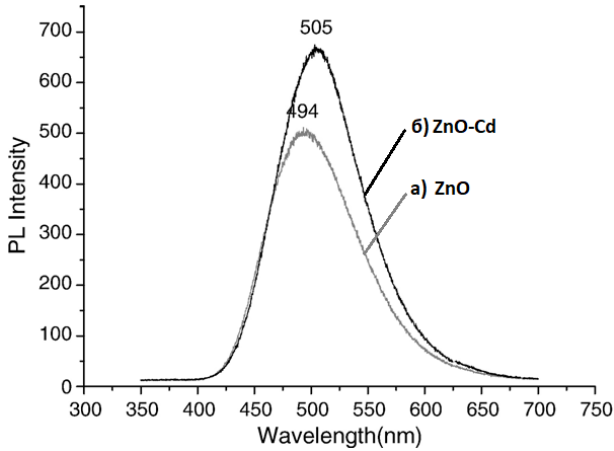


Fig. 15. PL spectra of undoped and Cd-doped ZnO nanostructures [44].

In Fig. 16, all samples show similar broad emission bands with different maxima associated with exciton recombination [29], edge emission (NBE), as well as maxima from transitions from deep defect levels, such as oxygen vacancy traps. The specific peak, its position and the corresponding mechanism observed in the resulting $Zn_{1-x}Cd_xO$ ($0 \leq x \leq 1$) structure are given in table 1.

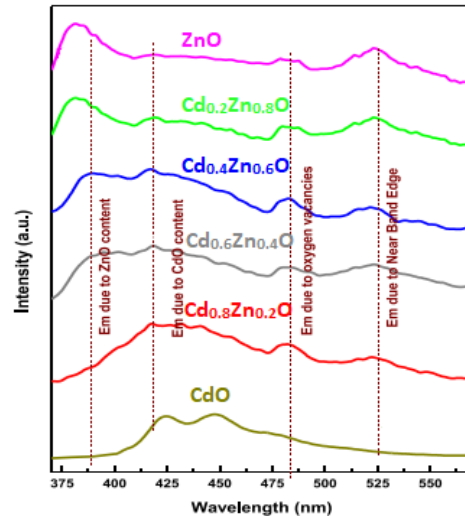


Fig. 16. PL spectra structure of $Cd_{1-x}Zn_xO$ ($0 \leq x \leq 1$) [45].

PL spectra of the $Zn_{1-x}Cd_xO$ structure with cadmium content $0 \leq x \leq 1$, can be seen in Fig. 20. More detailed information on PL mechanisms and peaks is given in table 1.

CdO sample has two peaks at 422 and 448 nm, which correspond to undoped CdO. Since CdO is a direct-band semiconductor nanomaterial, a slight shift of the exciton emission peaks is observed when substituted with zinc. In addition, with increasing Zn content, the emission edge by recombination of excitons in ZnO (sample $Zn_{0.2}Cd_{0.8}O$), shifts toward shorter wavelengths. In Fig. 16, it can be seen that the shift of the emission peak of CdO is insignificant compared to the shift of the exciton peak of ZnO [45].

Table 1.

Description of observed PL peaks in the structure $Zn_{1-x}Cd_xO$ ($0 \leq x \leq 1$) [1]

	Peaks of FL						Mechanism radiation
	CdO	$Cd_{0.8}Zn_{0.2}O$	$Cd_{0.6}Zn_{0.4}O$	$Cd_{0.4}Zn_{0.6}O$	$Cd_{0.2}Zn_{0.8}O$	ZnO	
1	–	–	387	382	380	378	The edge emission of undoped ZnO is associated with the recombination of excitons
2	422	420	419	417	415	–	The emission is associated with charge transfer in undoped CdO
3	448	–	–	–	–	–	The emission is associated with transitions of charge carriers from the defect level of internodal cadmium to the valence band
4	–	486	486	486	486	486	The emission is associated with the transitions of charge carriers from the defective level of internodal zinc to the valence band
5	–	520	520	520	520	520	The emission is associated with singly ionized oxygen vacancies (V_o) existing in $Zn_{1-x}Cd_xO$

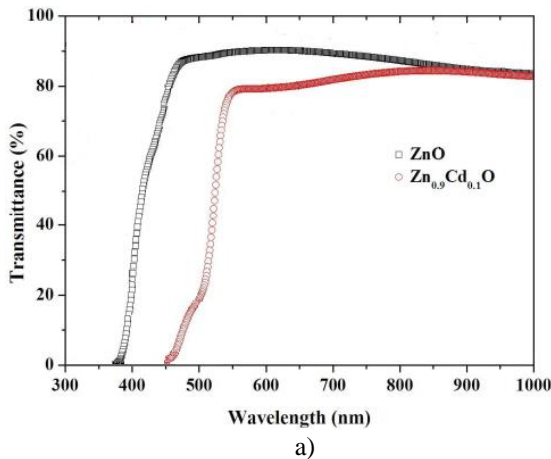
In Fig. 17 shows the transmission and absorption spectra of ZnO and Zn_{0.9}Cd_{0.1}O films, which were synthesized by the spin-coating method. It can be seen that both films have a transparency of 80-90 %. It was also found that cadmium doping causes a slight decrease in transmission in the visible region. ZnO-Cd film shows a shift of the absorption edge by about 80 nm compared to the ZnO film [30]. A similar result was obtained in [17], where the films were synthesized by pulsed laser deposition method.

Undoped ZnO shows absorption at 367 nm. This is shown in Fig. 18. After adding 5 % and 10 % Cd to ZnO, it shows a higher absorption band at 377 and 385 nm, respectively. Undoped ZnO and ZnO doped with cadmium have a large optical transmission window in the region of 400–800 nm. No visible absorption band was detected in this region. A wide transparency area is necessary for fabrication nanodevices and is applicable to optoelectronics.

The energy gap width (E_g) of undoped ZnO and Cd-doped ZnO nanoparticles is shown in Fig. 19, were calculated according to the formula:

$$E_g = \frac{hc}{\lambda} \quad (1)$$

where h – Planck's constant,



c – speed of light,
 λ – wavelength.

The appropriate values of the energy gap width of undoped ZnO and Cd-doped ZnO nanorods are shown in Fig. 19. It can be seen that with an increasing level of cadmium doping, the edge of the fundamental absorption decreases. The value of E_g for undoped ZnO is 3.24 eV. It decreases to 3.21 eV for ZnO doped with 5 % Cd and to 3.18 eV for ZnO doped with 10 % Cd. This decrease can be explained by the large difference in E_g values for zinc oxide and cadmium oxide [34,37,38,40].

The effect of an increased dose of doping, which was considered in [37] on optical properties, can be seen in Fig. 20 and Fig. 21.

Optical analysis in the wavelength range of 200–800 nm at room temperature of CdO-ZnO films deposited on a glass substrate is shown in Fig. 20, a. All films have a high transmittance in the visible area, which decreases with an increasing concentration of cadmium impurity. This change was a consequence of the large gap in electronic band structure of CdO and ZnO. The ZnO thin film has the highest transmittance, while the minimum transmittance was observed in the CdO film in the visible region.

From the dependence $(ah\nu)^2$ to $h\nu$ for the films shown in Fig. 20, b, received values of 2.10, 2.40, 3.01 and 3.20 eV. This sequence corresponds to thin films of CdO, No.1,

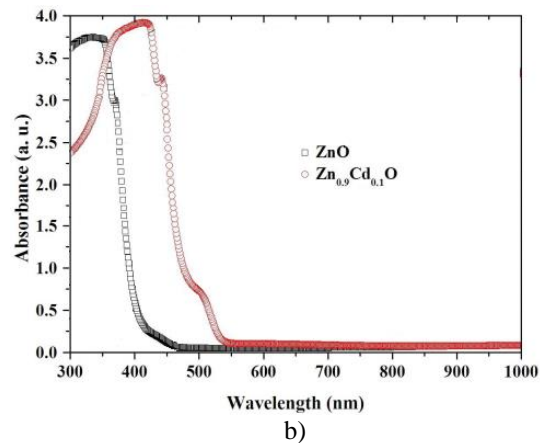


Fig. 17. Spectra of ZnO_{0.9}Cd_{0.1}O thin films : a) – optical transmission; b) – absorption spectra [41].

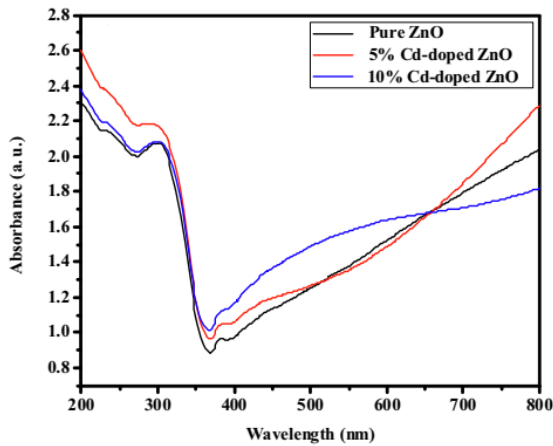


Fig.18. Absorption spectra of undoped and Cd-doped ZnO nanoparticles [42].

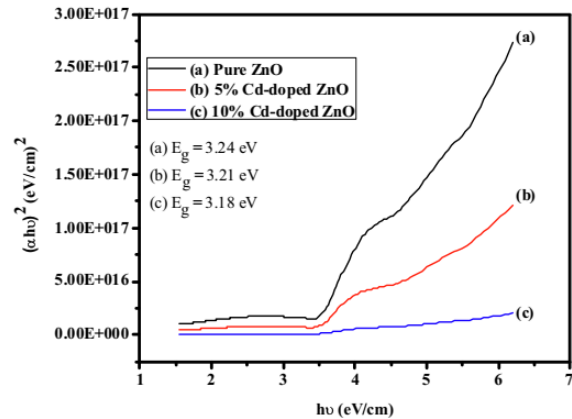


Fig. 19. The width of the energy gap of undoped and cadmium-doped ZnO synthesized by reflux method [42].

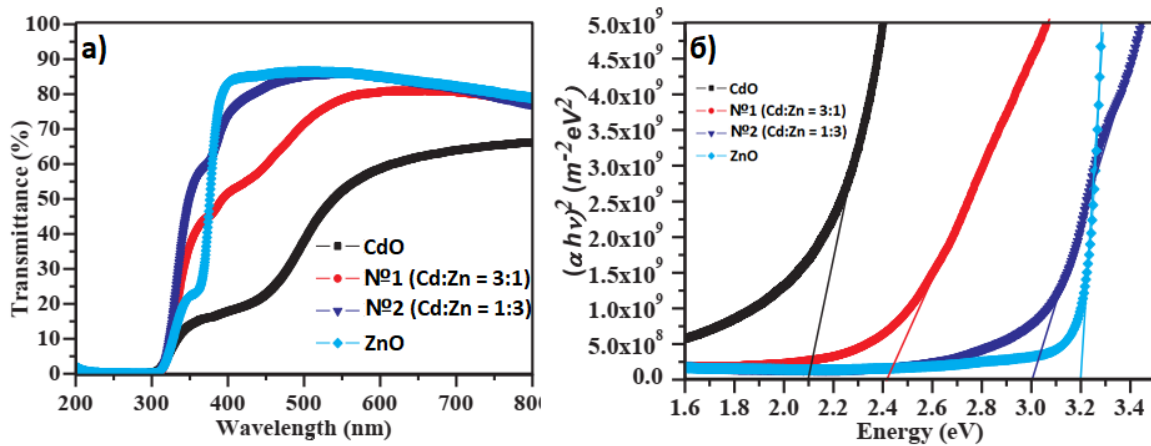


Fig. 20. Summary graphs of the optical characteristics of the obtained samples: a – optical transmission spectra; b – dependence of $(\alpha h\nu)^2$ to $h\nu$ [25].

No.2 and ZnO. The width of the energy gap is inversely proportional to the concentration of Cd in the thin film. The electron binding energy of CdO may be responsible for the narrowing of the bandgap because, due to the large atomic radius, conduction electrons require less energy to move into the valence band compared to ZnO.

PL spectra of CdO-ZnO at room temperature are shown in Fig. 21. Wide mission peaks were observed in the 380–440 nm region, which corresponds to excitonic emission near the band edge. The spectrum also shows emission in the visible region centered around 720 nm (red light), as shown in Fig. 21. The maximum intensity of the PL peak for red light was observed for thin film №1 with a ratio of Zn: Cd = 3:1. This emission occurs due to the transition of electrons from the bottom of the conduction zone to the level of vacancies - defects in the crystal structure of CdO and ZnO.

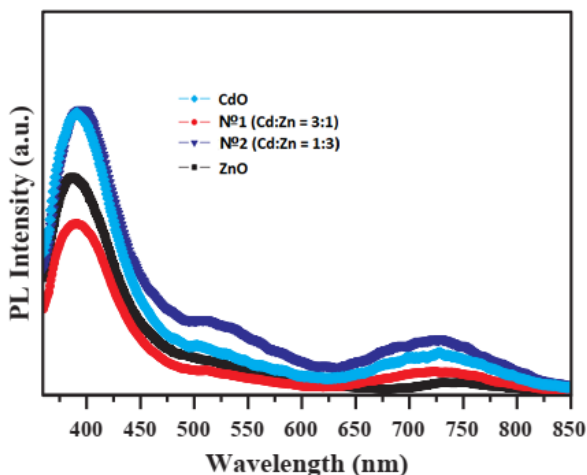


Fig.21. PL spectra of CdO-ZnO thin films [25].

It is also appropriate to consider the study optical properties of $\text{Zn}_{1-x}\text{Cd}_x\text{O}$ thin films in the article [36], in particular to investigate the spectra of optical transmittance and the dependence of $(\alpha h\nu)^2$ to $h\nu$ for the films that were deposited by spray pyrolysis method. The corresponding curves are shown in Fig. 22.

Comparing the graphs shown in Fig. 20, a, and Fig. 22, a, you can see the similarity of the results obtained by

different methods and at different doping concentrations. In addition, films synthesized by the spray pyrolysis method show greater transparency in the ultraviolet spectrum (Fig. 22, a, c).

Thin films were deposited by synthesized by the DC and RF reactive magnetron co-sputtering $\text{Zn}_{1-x}\text{Cd}_x\text{O}$ in the article [30]. The peculiarity of this work is that it used two metal targets made of undoped zinc and cadmium. 80 W was applied to the zinc target and to modulate the molar fraction of cadmium in the structure, the power applied to the cadmium target was varied from 0 to 120 W. Table 2 shows the ratio of the composition of elements in $\text{Zn}_{1-x}\text{Cd}_x\text{O}$ films applied at different powers of sputtering a cadmium target (P_{Cd}). Using the method of energy dispersive X-ray spectroscopy, it was found that the Cd content increases with an increase P_{Cd} .

As a result of increasing the proportion of cadmium in the structure, the width of the energy gap decreases. This is demonstrated in Fig. 23.

On the basis of all considered materials and synthesis methods, a summary table can be compiled that will demonstrate the effect of cadmium doping on the width of the energy gap (Table 3).

2.3 Photocatalytic activity

Photocatalysis appears to be an interesting approach to water purification with the possibility of using sunlight as a sustainable and renewable energy source (Fig. 24). This technology is based on the use of a semiconductor that can be excited by light with an energy higher than the band gap, inducing the formation of electron-hole pairs that can participate in redox reactions. Nanoscale semiconductors typically have high activity and high degree of functionality, large specific surface area, and size-dependent properties, which making them suitable for water treatment applications.

In recent years, most photocatalysts have been specifically designed for applications under sunlight, but many researchers have focused their attention on UV-active systems. Thus, nanoscale semiconductors sensitive to UV and visible or sunlight should be considered.

Some publications have demonstrated a better photoresponse for ZnO compared to TiO_2 for the photocatalytic decomposition of some dyes in water [43].

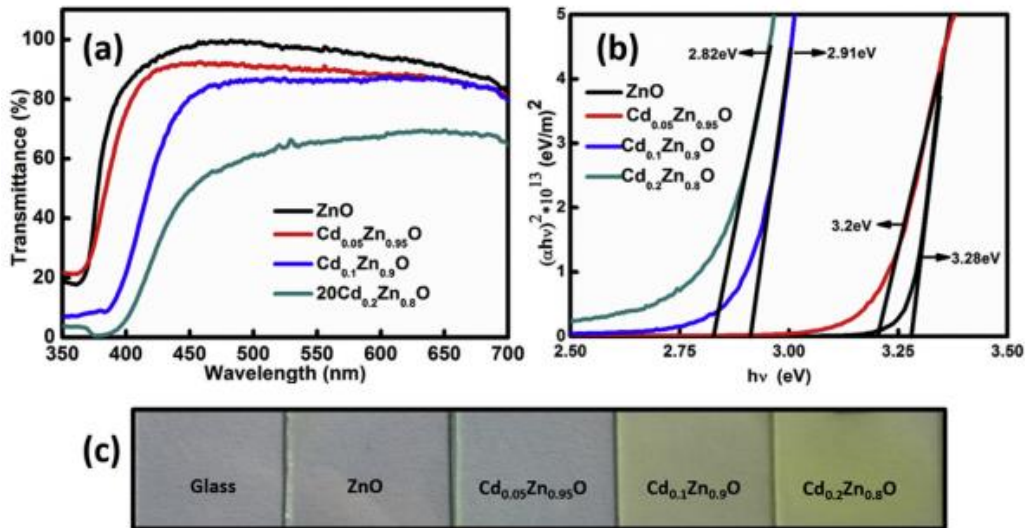


Fig. 22. Optical transmission spectra (a), dependence $(ahv)^2$ to hv (b) and appearance of deposited $Zn_{1-x}Cd_xO$ thin films (c) [35].

Table 2. Composition of $Zn_{1-x}Cd_xO$ films according to energy dispersive analysis [30] **Ошибка! Закладка не определена.**

$P_{Cd,W}$	Atomic fraction, %		
	O	Zn	Cd
20	50.68	48.67	0.65
40	51.24	47.45	1.31
60	51.59	46.07	2.34
120	51.99	40.48	7.53

Table 3. Comparative analysis of different doping concentrations and different synthesis methods [18]

Cadmium content in the film $Zn_{1-x}Cd_xO$, %	Synthesis technique	Band gap width, eV	Link
$x = 0.45$ atomic	Sol-gel method	3.20	[28]
$x = 0.51$ atomic		3.19	
$x = 0.56$ atomic		3.15	
$x = 16$ atomic	Pulsed laser deposition	2.75	[17]
$x = 25$ atomic		2.4	
$x = 50$ atomic		2.19	
$x = 10$ atomic	Sol-gel spin coating	2.66	[41]
$x = 5$ molar	Reflux method	3.21	[42]
$x = 10$ molar		3.18	
$x = 67$ voluminous	Sol-gel spin coating method	2.4	[25]
$x = 33$ voluminous		3	
$x = 0.65$ atomic	High-frequency reactive magnetron sputtering	3.21	[30]
$x = 31$ atomic		3.16	
$x = 2.34$ atomic		3.07	
$x = 7.53$ atomic		2.82	
$x = 5$ atomic	Pulsed laser deposition	3.2	[19]
$x = 10$ atomic		2.97	
$x = 5$ atomic	Spray pyrolysis method	3.2	[35]
$x = 10$ atomic		2.91	
$x = 20$ atomic		2.82	

Several literature studies determined the method of doping ZnO-Cd to achieve a good photocatalytic effect. Despite this, the properties and the mechanism behind have not been fully explained [43]. It should be noted that the improvement of photocatalytic efficiency is closely

related to structural properties, such as morphology, particle size, crystal orientation, degree of crystallization and oxygen defects, which greatly affect the activity and stability of photocatalysts [44].

Effect of doping with Cd ions on the photocatalytic

properties of ZnO nanoparticles obtained by the deposition method is described in [47].

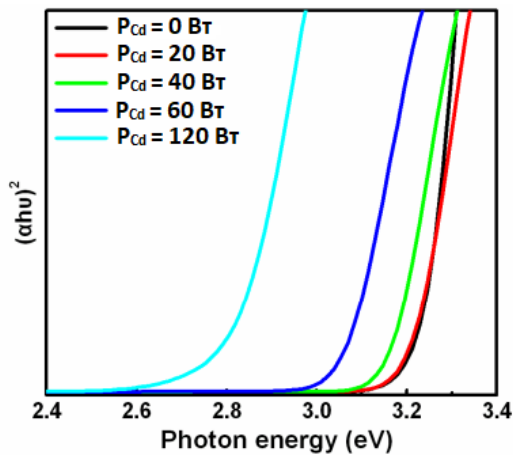


Fig. 23. Dependences $(\alpha hv)^2$ to $h\nu$ for $Zn_{1-x}Cd_xO$ films at different sputtering powers of the cadmium target [30].

To study the photocatalytic activity of ZnO-Cd nanostructures, the absorption spectra obtained during the degradation of crystal violet in an aqueous solution at ambient temperature were used (Fig. 25). The dye solution containing photocatalyst was exposed to UV irradiation with a 6 W mercury lamp and samples were collected at regular intervals to determine the photocatalytic behavior. The sample was centrifuged for 3 minutes at 2500 rpm to separate the catalyst particles from the aqueous phase to determine the degree of discoloration.

In Fig. 25, and in the Table 3 shows the percentage degradation of crystal violet for undoped ZnO and Cd doped ZnO with different molar fractions during 120 min of illumination.

The results showed that the best dye degradation in cadmium-doped ZnO catalysts occurs in the following order: 0.5 mol %, 0 mol %, 2 mol %, 1.5 mol %, 1.0 mol % cadmium doping. It can be concluded that the

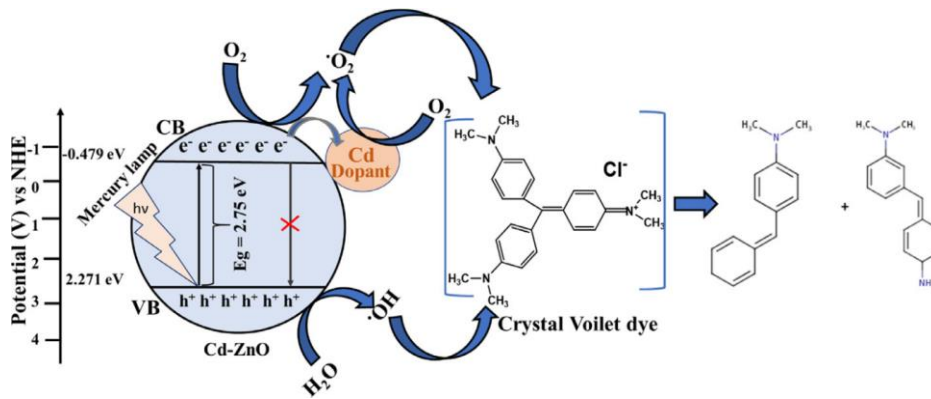


Fig. 24. Photocatalytic mechanism of degradation of crystal violet using ZnO - Cd nanoparticles [47].

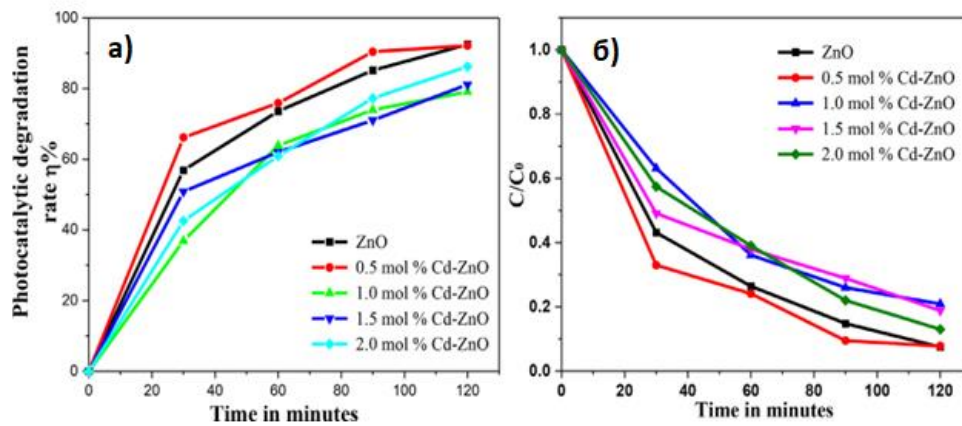


Fig. 25. a – diagram of photocatalytic degradation of crystal violet depending on the time of irradiation; b – a graph of the dependence of the concentration of crystal violet at different molar ratios of ZnO doped with Cd [47].

Table 3.

Influence of molar fraction of cadmium on photodegradation of samples [47]

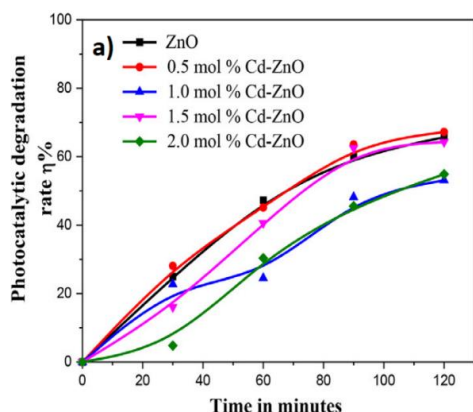
		Duration of photocatalysis, min			
		30	60	90	120
		Biodegradation, %			
Molar fraction of Cd, mol %	Cd = 0 %	56.88	73.57	85.17	92.47
	Cd = 0.5 %	66.14	75.87	90.4	92.13
	Cd = 1 %	36.88	63.85	73.94	79.08
	Cd = 1.5 %	5.82	62.0	71.0	81.0
	Cd = 2 %	42.56	60.91	77.24	86.23

implantation of 0.5 mol % cadmium improves the photocatalytic activity of ZnO in the crystal violet due to the increased charge separation potential. Excessive inclusion of Cd leads to an increase in the rate of recombination of electrons and holes, which leads to a loss of photocatalytic activity. The authors of the article [47] suggested that this may be due to the presence of cadmium nanoparticles in the volume of zinc. The presence of a Cd impurity of more than 0.5 molar % in the photocatalyst leads to a decrease in the efficiency of the photocatalyst.

Undoped and cadmium doped ZnO samples were able to degrade the crystal violet dye, as seen by the decrease in concentration, which indicated that the chromophoric groups of the dye were converted to intermediate products. Fig. 25, b shows that more than 80 % of the dye decomposes within 120 minutes in ZnO-Cd nanoparticles.

The results in Fig. 26, and showed that nanoparticles of the ZnO-Cd series can destroy approximately from 53 to 67 % of alizarin red (AR) dye during irradiation with an ultraviolet lamp. In Fig. 26, it is shown that a significant decomposition was observed in the ultraviolet in the absence of a catalyst. The rate of decomposition reached 84 % in 120 minutes. These results show that a series of ZnO-Cd compounds can be effectively used to destroy cationic dyes, but not anionic ones.

The work also investigated the influence of the



catalyst dose in the range from 0.5 mg to 3.0 mg on the decomposition of crystal violet. In the Table 4 shows the efficiency of dye degradation. Increasing the amount of catalyst in the range from 0.5 mg to 2.0 mg led to an increase in photocatalytic degradation. This suggests that the rate of degradation improves with increasing amount of catalyst. In turn, this result can be caused by an increase in the number of active centers on the surface of the catalyst. Since a higher dose of catalyst blocks the rays of the ultraviolet lamp from penetrating the solution, it also leads to a decrease in catalytic activity.

The pH level is one of the most important factors that can affect the process of dye degradation on the surface of the photocatalyst. The influence of different pH values in the range from 2 to 12 (in acidic, neutral and alkaline pH environments) on the efficiency of dye degradation was investigated. The obtained dependencies were presented in the Table 5.

In an acidic environment, the degradation efficiency of crystal violet was 90%, but in an alkaline environment it was higher and amounted to 100 % for 12 pH (Fig. 27). The efficiency of crystal violet decomposition was increased from 85% at pH 8 to 100% at pH 10 in pure ZnO solution. 100% decomposition was achieved in less than 60 min at pH 12. During the same time, 0.5 mol % Cd in the ZnO structure allows the dye to be decomposed by

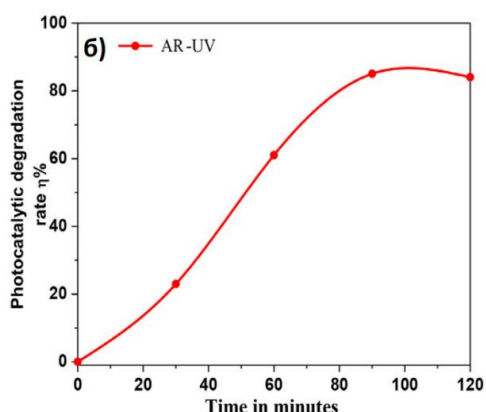


Fig. 26. Percentage diagram of the photocatalytic decomposition of alizarin red with: a – different concentration of the catalyst in UV; b – only in UV without catalyst [47].

Table 4.

Influence of the catalyst content on the photodegradation of samples [47]

		Duration of photocatalysis, min			
		30	60	90	120
		Biodegradation, %			
Catalyst content, mg	0,5	69.2	77.6	87.2	90.4
	1	66.14	75.87	90.4	92.15
	2	79.6	86.2	95.6	100
	3	69.6	77.7	88.5	88.5

Table 5.

Influence of the acidity of the medium on photodegradation of samples [47]

		Duration of photocatalysis, min			
		30	60	90	120
		Biodegradation, %			
pH level	2	71.28	82.12	88.26	92.15
	4	48.62	73.39	83.3	93.76
	6	44	80	85.13	86.23
	8	59.81	85.87	88.44	94.31
	10	64.4	100	100	100
	12	100	100	100	100

approximately 94 % at pH 8, 100% at pH 10 and 12 in 60 and 30 minutes respectively.



Fig. 27. Results of photodegradation of crystal violet [47].

From the Table 4 and 5 clearly show that 2 mg of the catalyst doped with 0.5 mol % Cd at pH 10 and 12 have a higher decomposition efficiency for 60 min and 30 min compared to 1, 1.5 and 2 mol % Cd in the ZnO structure.

The photocatalytic activity was also studied in the article [23]. ZnO and ZnO-Cd nanoparticles were synthesized by the hydrothermal method.

The photocatalytic activity of hydrothermally synthesized ZnO doped with cadmium was evaluated by testing the degradation of rhodamine B. The diagram of the decomposition of the ZnO-Cd photocatalyzed dye is shown in Fig. 28. Also, for comparison, a graph of dye decay on a sample of undoped ZnO is given. The time diagrams demonstrate a significant enhancement of the photocatalytic activity when ZnO is doped with cadmium using the hydrothermal method.

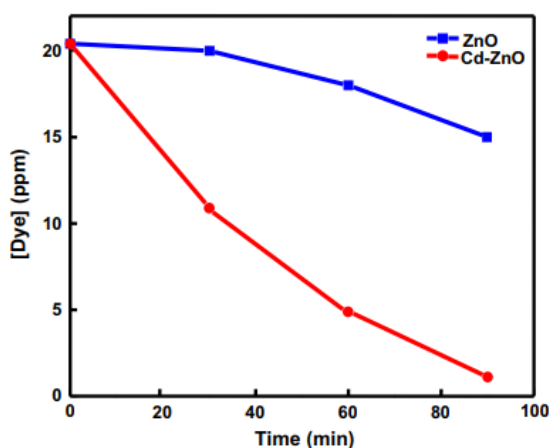


Fig. 28. Photocatalytic degradation of rhodamine B [23].

In Fig. 29 residual concentration of methylene blue (MB) was obtained for all samples and compared with the results decomposition of MB without a photocatalyst. It was observed that the MB dye decomposed by 99% within 180 minutes using the $Cd_{0.2}Zn_{0.8}O$ sample as catalyst, while only 28, 48, 65, 88 and 94 % of the dye decomposed when the zinc samples were used $x = 0; 0.2; 0.4; 0.6$ and 1 in $Cd_{1-x}Zn_xO$, respectively, as a catalyst under the same experimental conditions [45].

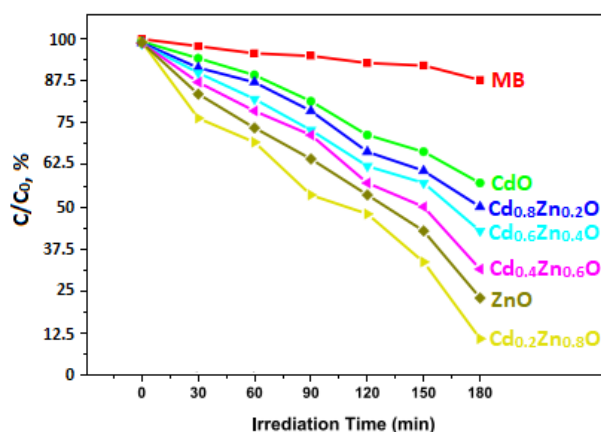


Fig.29. Graph of the residual concentration of methylene blue (MB) during photocatalysis by structures with different content of cadmium doping [45].

Conclusions

Materials based on ZnO and cadmium, are gaining increased attention as promising photocatalytic material and can be successfully applied for organic dyes degradation. This review considers the influence of cadmium doping on morphology, structure and optical properties of ZnO obtained by various techniques. It was discussed that Cd-doping modifies the characteristics of ZnO and enhances its suitability for photocatalysis due to suppressing the recombination rate of electron-hole pairs, increasing charge separation efficiency, and improving the production rate of hydroxyl radicals. The band engineering of ZnO toward visible range by Cd-doping leads to the increased ability to absorb more irradiation of the solar spectrum. Additional research is needed to evaluate how photocatalyst properties of Cd-doped ZnO correlate with their optical properties. It was shown that Cd-doped ZnO is the perspective multifunctional material for wide-scale environmental, technological, and biomedical applications.

Acknowledgements

This work was supported by the project of research works of young scientists of NAS of Ukraine "Creation of effective photocatalytic materials based on ZnO-Cd system for water purification from organic pollutants".

Didus R.I. – Senior Engineer of Department of Physics and Technology of Photoelectronic and Magnetoactive Materials;

Myroniuk D.V. – Candidate of Physical and Mathematical Sciences, Senior Researcher of Department of Physics and Technology of Photoelectronic and Magnetoactive Materials;

Myroniuk L.A. – Candidate of Chemical Sciences, Researcher of Department of Physics and Technology of Photoelectronic and Magnetoactive Materials;

Ievtushenko A.I. – Candidate of Physical and Mathematical Sciences, Senior Researcher, Head of Department of Physics and Technology of Photoelectronic and Magnetoactive Materials.

- [1] O. E. Baibara, M.V. Radchenko, V.A. Karpyna, A.I. Ievtushenko, *A Review of the Some Aspects for the Development of ZnO Based Photocatalysts for a Variety of Applications*, Physics and Chemistry of Solid State, 22 (3), 585 (2021); <https://doi.org/10.15330/pcss.22.3.585-594>.
- [2] S. P. Hoffmann, C. Meier, T. Zentgraf, W.-G. Schmidt, H. Herrmann, *Zinc-Oxide Based Photonic Crystal Membranes*, University of Paderborn, (2018).
- [3] A. Antony, I. V. Kityk, G. Myronchuk, G. Sanjeev, V. C. Petwal, V. P. Verma, J. Dwivedi, *A study of 8 meV e-beam on localized defect states in ZnO nanostructures and its role on photoluminescence and third harmonic generation*, Journal Lumin, 207, 321 (2019); <https://doi.org/10.1016/j.jlumin.2018.11.043>.
- [4] A. Sevik, B. Coskun, M. Soylu, *The effect of molar ratio on the photo-generated charge activity of ZnO–CdO composites*, Eur. Phys. J., 135, 65 (2020); <https://doi.org/10.1140/epjp/s13360-020-00129-w>.
- [5] Rahman, *Zinc oxide light-emitting diodes: a review*, Opt. Eng., 58(1), 010901 (2019); <https://doi.org/10.1117/1.OE.58.1.010901>.
- [6] Y. J. Noh, J. G. Kim, S. S. Kim, H. K. Kim, S. I. Na, *Efficient semitransparent perovskite solar cells with a novel indium zinc tin oxide top electrode grown by linear facing target sputtering*, Journal of Power Sources. 437, 226894 (2019); <https://doi.org/10.1016/j.jpowsour.2019.226894>.
- [7] S. Golovynskyi, A. Ievtushenko, S. Mamykin, M. Dusheiko, I. Golovynska, O. Bykov, O. Olifan, D. Myroniuk, S. Tkach, J. Qu, *High transparent and conductive undoped ZnO thin films deposited by reactive ion-beam sputtering*, Vacuum, 153, 204 (2018); <https://doi.org/10.1016/j.vacuum.2018.04.019>.
- [8] M. Pirsaeheb, H. Hossaini, N. Simin, A. Nahid, S. Behzad, K. Toba, *Optimization of photocatalytic degradation of methyl orange using immobilized scoria-Ni/TiO₂ nanoparticles*, Journal of Nanostructure in Chemistry, 10, 143 (2020); <https://doi.org/10.1007/s40097-020-00337-x>.
- [9] V. Karpyna, A. Ievtushenko, O. Kolomys, O. Lytvyn, V. Strelchuk, V. Tkach, S. Starik, V. Baturin, O. Karpenko, *Raman and Photoluminescence Study of Al,N-Codoped ZnO Films Deposited at Oxygen-Rich Conditions by Magnetron Sputtering*, Phys. Status Solidi B., 257, 1900788 (2020); <https://doi.org/10.1002/pssb.201900788>.
- [10] A. Ievtushenko, O. Khyzhun, I. Shtepliuk, O. Bykov, R. Jakiela, S. Tkach, E. Kuzmenko, V. Baturin, O. Karpenko, O. Olifan, G. Lashkarev, *X-Ray photoelectron spectroscopy study of highly-doped ZnO:Al,N films grown at O-rich conditions*, Journal of Alloys and Compounds, 722, 683 (2017); <https://doi.org/10.1016/j.jallcom.2017.06.169>.
- [11] E. Mosquera, I. del Pozo, M. Morel, *Structure and redshift of optical band gap in CdO–ZnO nanocomposite synthesized by the sol-gel method*, Journal of Solid State Chemistry, 203, 265 (2013); <https://doi.org/10.1016/j.jssc.2013.08.025>.
- [12] E. Ozugurlu, *Cd-doped ZnO nanoparticles: An experimental and first-principles DFT studies*, Journal of Alloys and Compounds, 861, 158620 (2020); <https://doi.org/10.1016/j.jallcom.2021.158620>.
- [13] I. Shtepliuk, G. Lashkarev, V. Khomyak, P. Marianchuk, P. Koreniuk, D. Myroniuk, V. Lazorenko, I. Timofeeva, *Effects of Ar/O₂ Gas Ratio on the Properties of the Zn_{0.9}Cd_{0.1}O Films Prepared by DC Reactive Magnetron Sputtering*, Acta Physica Polonica A, 120, A-61 (2011); <https://doi.org/10.12693/APhysPolA.120.A-61>.
- [14] I. Shtepliuk, V. Khranovskyy, G. Lashkarev, V. Khomyak, V. Lazorenko, A. Ievtushenko, ... & R. Yakimova, *Electrical properties of n-Zn_{0.94}Cd_{0.06}O/p-SiC heterostructures*, Solid-State Electronics, 81, 72-77 (2013); <https://doi.org/10.1016/j.sse.2013.01.015>.
- [15] S.Y. Lee, Y. Li, J.S. Lee, J.K. Lee, M. Nastasi, S.A. Crooker, ... & J.S. Kang, *Effects of chemical composition on the optical properties of Zn 1– x Cd x O thin films*, Applied physics letters, 85(2), 218-220 (2004); <https://doi.org/10.1063/1.1771810>.
- [16] P. Misra, P. K. Sahoo, P. Tripathi, V. N. Kulkarni, R. V. Nandedkar, L. M. Kukreja, *Sequential pulsed laser deposition of Cd_xZn_{1-x}O alloy thin films for engineering ZnO band gap*, Appl. Phys. A, 78, 37 (2004); <https://doi.org/10.1007/s00339-003-2296-0>.
- [17] L. N. Bai, B. J. Zheng, J. S. Lian, Q. Jiang, *First-principles calculations of Cd-doped ZnO thin films deposited by pulse laser deposition*, Solid State Sciences, 14, 698 (2012); <https://doi.org/10.1016/j.solidstatesciences.2012.03.018>.
- [18] S. Sharma, B. Saini, R. Kaur, M. Tomar, V. Gupta, A. Kapoor, *Low resistivity of pulsed laser deposited Cd_xZn_{1-x}O thin films*, Ceramics International, 45, 1900 (2019); <https://doi.org/10.1016/j.ceramint.2018.10.082>.
- [19] S. Chen, Q. Li, I. Ferguson, T. Lin, L. Wan, Z. C. Feng, L. Zhu, Z. Ye, *Spectroscopic ellipsometry studies on ZnCdO thin films with different Cd concentrations grown by pulsed laser deposition*, Applied Surface Science, 42, 383 (2017); <https://doi.org/10.1016/j.apsusc.2017.02.264>.
- [20] M. Tortosa, M. Mollar, B. Mari, *Synthesis of ZnCdO thin films by electrodeposition*, Journal of Crystal Growth, 304, 97 (2007); <https://doi.org/10.1016/j.jcrysgro.2007.02.010>.
- [21] O. Lupan, T. Pauporté, L. Chow, G. Chai, B. Viana, V. V. Ursaki, E. Monaico, I. M. Tiginyanu, *Comparative study of the ZnO and Zn_{1-x}Cd_xO nanorod emitters hydrothermally synthesized and electrodeposited on p-GaN*, Applied Surface Science, 259, 399 (2012); <https://doi.org/10.1016/j.apsusc.2012.07.058>.
- [22] S.-I. Park, Y. -J. Quan, S. -H. Kim, H. Kim, S. Kim, D. -M. Chun, S. -H. Ahn, *A review on fabrication processes for electrochromic devices*, International Journal of Precision Engineering and Manufacturing-Green Technology, 3, 397 (2016); <https://doi.org/10.1007/s40684-016-0049-8>.

- [23] C. Karunakaran, A. Vijayabalan, G. Manikandan, *Photocatalytic and bactericidal activities of hydrothermally synthesized nanocrystalline Cd-doped ZnO*, Superlattices and Microstructures, 5, 443 (2012); <https://doi.org/10.1016/j.spmi.2012.01.008>.
- [24] Y. Caglar *Morphological, optical and electrical properties of CdZnO films prepared by sol-gel method* Journal of Physics D: Applied Physics, 42, 065421 (2009); <http://dx.doi.org/10.1088/0022-3727/42/6/065421>.
- [25] J. K. Rajput, T. K. Pathak, V. Kumar, H. C. Swart, L. P. Purohit, *CdO:ZnO nanocomposite thin films for oxygen gas sensing at low temperature*, Materials Science and Engineering: B., 228, 241 (2018); <https://doi.org/10.1016/j.mseb.2017.12.002>.
- [26] F. Yakuphanoglu, S. Ilican, M. Caglar, Y. Caglar, *Microstructure and electro-optical properties of sol-gel derived Cd-doped ZnO films*, Superlattices and Microstructures, 47, 732 (2010); <https://doi.org/10.1016/j.spmi.2010.02.006>.
- [27] T. K. Pathak, J. K. Rajput, V. Kumar, L. P. Purohit, H. C. Swart, R. E. Kroon, *Transparent conducting ZnO-CdO mixed oxide thin films grown by the sol-gel method*, Journal of Colloid and Interface Science, 487, 378 (2017); <https://doi.org/10.1016/j.jcis.2016.10.062>.
- [28] N. Kumar, A. Srivastava, *Faster photoresponse, enhanced photosensitivity and photoluminescence in nanocrystalline ZnO films suitably doped by Cd*, Journal of Alloys and Compounds, 706, 438 (2017); <http://dx.doi.org/10.1016/j.jallcom.2017.02.244>.
- [29] I. Shteplyuk, V. Khranovskyy, G. Lashkarev, V. Khomyak, A. Ievtushenko, V. Tkach, V. Lazorenko, I. Timofeeva, R. Yakimova, *Microstructure and luminescence dynamics of ZnCdO films with high Cd content deposited on different substrates by DC magnetron sputtering*, Applied Surface Science, 276, 550 (2013); <https://doi.org/10.1016/j.apsusc.2013.03.132>.
- [30] Y. R. Sui, Y. J. Wu, Y. P. Song, S. Q. Liv, B. Yao, X. W. Meng, L. Xiao, *A study on structural formation and optical properties of Zn_{1-x}Cd_xO thin films synthesized by the DC and RF reactive magnetron co-sputtering*, Journal of Alloys and Compounds, 678, 383 (2016); <https://doi.org/10.1016/j.jallcom.2016.03.302>.
- [31] A. Ievtushenko, V. Tkach, V. Strelchuk, L. Petrosian, O. Kolomys, O. Kutsay, V. Garashchenko, O. Olifan, S. Korichev, G. Lashkarev, V. Khranovskyy, *Solar Explosive Evaporation Growth of ZnO Nanostructures*, Applied Science, 7(4), 383 (2017); <https://doi.org/10.3390/app7040383>.
- [32] S. Vijayalakshmi, S. Venkataraj, R. Jayavel, *Characterization of cadmium doped zinc oxide (Cd:ZnO) thin films prepared by spray pyrolysis method*, Journal of Physics D: Applied Physics, 41, 7 (2008); <http://dx.doi.org/10.1088/0022-3727/41/24/245403>.
- [33] D. Acharya, S. Moghe, R. Panda, S. B. Shrivastava, M. Gangrade, T. Shripathi, D. M. Phase, V. Ganesan, *Effect of Cd dopant on electrical and optical properties of ZnO thin films prepared by spray pyrolysis route*, Thin Solid Films, 525, 49 (2012); <https://doi.org/10.1016/j.tsf.2012.10.100>.
- [34] N. L. Tarwal, A. R. Patil, N. S. Harale, A. V. Rajgure, S. S. Suryavanshi, W. R. Bae, P. S. Patil, J. H. Kim, J. H. Jang, *Gas sensing performance of the spray deposited Cd-ZnO thin films*, Journal of Alloys and Compounds, 598, 282 (2014); <https://doi.org/10.1016/j.jallcom.2014.01.200>.
- [35] S. P. Bharath, K. V. Bangera, G. K. Shivakumar, *Properties of Cd_xZn_{1-x}O thin films and their enhanced gas sensing performance*, Journal of Alloys and Compounds, 720, 39 (2017); <http://dx.doi.org/10.1016/j.jallcom.2017.05.240>.
- [36] Q. Wan, Q. H. Li, Y. J. Chen, T. H. Wang, X. L. He, X. G. Gao, J. P. Li, *Positive temperature coefficient resistance and humidity sensing properties of Cd-doped ZnO nanowires*, Appl. Phys. Lett, 84, 3085 (2004); <https://doi.org/10.1063/1.1707225>.
- [37] S. Sakurai, T. Kubo, D. Kajita, T. Tanabe, H. Takasu, S. Fujita, S. Fujita, *Blue Photoluminescence from ZnCdO Films Grown by Molecular Beam Epitaxy*, Japanese Journal of Applied Physics, 39, 1146 (2000); <http://dx.doi.org/10.1143/JJAP.39.L1146>.
- [38] S. Shigemori, A. Nakamura, J. Ishihara, T. Aoki, J. Temmyo, *Zn_{1-x}Cd_xO film growth using remote plasma-enhanced metalorganic chemical vapor deposition*, Japanese Journal of Applied Physics, 43(8), 1088 (2004); <http://dx.doi.org/10.1143/JJAP.43.L1088>.
- [39] M. Souissi, A. Fouzri, G. Schmerber, *Highlighting of ferromagnetism above room temperature in Cd-doped ZnO thin films grown by MOCVD*, Solid State Communications, 218, 40 (2015); <https://doi.org/10.1016/j.ssc.2015.06.013>.
- [40] S. Mondal, P. Mitra, *Preparation of cadmium-doped ZnO thin films by SILAR and their characterization*, Bulletin of Materials Science, 35, 751 (2012); <https://doi.org/10.1007/s12034-012-0350-2>.
- [41] Jacob, L. Balakrishnan, S. R. Meher, K. Shambavi, Z. C. Alex, *Structural, optical and photodetection characteristics of Cd alloyed ZnO thin film by spin coating*, Journal of Alloys and Compounds, 695, 3753 (2017); <https://doi.org/10.1016/j.jallcom.2016.11.265>.
- [42] U. D. Babar, N. M. Garad, A. A. Mohite, B. M. Babar, H. D. Shelke, P. D. Kamble, U. T. Pawar, *Study the photovoltaic performance of pure and Cd-doped ZnO nanoparticles prepared by reflux method*, Materials Today: Proceedings, 43, 2780 (2021); <https://doi.org/10.1016/j.matpr.2020.08.008>.
- [43] G. K. Weldegebriael, *Synthesis method, antibacterial and photocatalytic activity of ZnO nanoparticles for azo dyes in wastewater treatment: A review*, Inorganic Chemistry Communications. 120, 108140 (2020); <https://doi.org/10.1016/j.inoche.2020.108140>.
- [44] Z. Liu, P. X. Yan, G. H. Yue, J. B. Chang, R. F. Zhuo, D. M. Qu, *Controllable synthesis of undoped/Cd-doped*

- ZnO nanostructures*, Materials Letters, 60, 3122 (2006); <https://doi.org/10.1016/j.matlet.2006.02.056>.
- [45] C. Bhukkal, R. Vats, B. Goswami, N. Rani, R. Ahlawat, *Zinc content (x) induced impact on crystallographic, optoelectronic, and photocatalytic parameters of Cd_{1-x}Zn_xO (0 ≤ x ≤ 1) ternary nanopowder*, Materials Science and Engineering: B., 265, 11500 (2021); <https://doi.org/10.1016/j.mseb.2020.115001>.
- [46] C. Belver, J. Bedia, A. Gómez-Avilés, M. Peñas-Garzón, J. J. Rodríguez, *Semiconductor photocatalysis for water purification in micro and nano technologies*, Nanoscale Materials in Water Purification, 581 (2019); <https://doi.org/10.1016/B978-0-12-813926-4.00028-8>.
- [47] F. Sanakousar, C. C. Vidyasagar, V. M. Jiménez-Pérez, B. K. Jayanna, Mounesh, A. H. Shridhar, K. Prakash, *Efficient photocatalytic degradation of crystal violet dye and electrochemical performance of modified MWCNTs/Cd-ZnO nanoparticles with quantum chemical calculations*, Journal of Hazardous Materials Advances, 2, 100004 (2021); <https://doi.org/10.1016/j.hazadv.2021.100004>.
- [48] H. A. Azqhandi, B. F. Vasheghani, F. H. Rajabi, M. Keramati, *Synthesis of Cd doped ZnO/CNT nanocomposite by using microwave method: Photocatalytic behavior, adsorption and kinetic study*, Results in Physics, 7, 1106 (2017); <https://doi.org/10.1016/j.rinp.2017.02.033>.

Р. І. Дідусь, Д. В. Миронюк, Л. А. Миронюк, А. І. Євтушенко

Особливості технологічного синтезу та властивості матеріалів на основі ZnO-Cd для фотокаталітичного застосування.

Огляд

Інститут проблем матеріалознавства ім. І.М. Францевича НАН України, Київ, Україна, romanik619@gmail.com

У цьому огляді узагальнено поточний стан матеріалів на основі ZnO-Cd для фотокаталітичних застосувань. Розглядаються відповідні технологічні методи синтезу, такі як імпульсне лазерне осадження, магнетронне розпилення, електроосадження, золь-гель, металоорганічне хімічне осадження з парової фази, випаровування, розпилювальний піроліз, а також останні розробки в ефективній та відтворюваній технології синтезу нано- та мікроструктурованого оксиду цинку, обговорюються леговані кадмієм тверді розчини Zn_{1-x}Cd_xO для фоторозпаду молекул органічних забруднювачів. Технологія синтезу та рівень легування кадмієм істотно впливає на структуру та морфологію оксиду цинку і, як наслідок, на оптичні та фотокаталітичні властивості. Показники добротності, теоретичні обмеження та раціональний контроль концентрації легуючої домішки кадмію необхідні для створення матеріалу зі збалансованими оптичними властивостями та фотокаталітичною активністю. Нарешті, важливість легування ZnO ізовалентною домішкою Cd значно покращує його фотокаталітичні властивості за рахунок звуження забороненої зони, зниження швидкості рекомбінації електронно-діркових пар, що підвищує ефективність просторового розділення зарядів, утворення активних оксидних радикалів і збільшення питомої поверхні. Таким чином, матеріали на основі ZnO-Cd є найбільш перспективними фотокаталітичними матеріалами для органічних забруднювачів.

Ключові слова: оксид цинку; легування кадмієм; морфологія; наноструктури; оптичні властивості; фотокаталіз.